Phosphorylation Regulates Transcriptional Activity of PAX3/FKHR and Reveals Novel Therapeutic Possibilities

Ralf Amstutz,[1] Marco Wachtel,[1] Heinz Troxler,[2] Peter Kleinert,[2] Margret Ebauer,[1] Torsten Haneke,[1] Christoph Oehler-Jänne,[3] Doriano Fabbro,[4] Felix K. Niggli,[1] and Beat W. Schäfer[1]

[1]Department of Oncology and [2]Division of Clinical Chemistry and Biochemistry, University Children's Hospital; [3]Division of Radiation Oncology, University Hospital Zurich, Zurich, Switzerland and [4]Novartis Pharma, Basel, Switzerland

Abstract

Inhibition of constitutive active signaling pathways, which are a characteristic phenomenon for many tumors, can be an effective therapeutic strategy. In contrast, oncogenic transcription factors, often activated by mutational events, are in general less amenable to small-molecule inhibition despite their obvious importance as therapeutic targets. One example of this is alveolar rhabdomyosarcoma (aRMS), in which specific translocations lead to the formation of the chimeric transcription factor PAX3/FKHR. Here, we found unexpectedly that the transcriptional activity of PAX3/FKHR can be inhibited by the kinase inhibitor PKC412. This occurs via specific phosphorylation sites in the PAX3 domain, phosphorylation of which is required for efficient DNA-binding and subsequent transcriptional activity. Consequently, we show that PKC412 exerts a potent antitumorigenic potential for aRMS treatment both *in vitro* and *in vivo*. Our study suggests that posttranscriptional modifications of oncogenic transcription factors can be explored as a promising avenue for targeted cancer therapy. [Cancer Res 2008;68(10):3767–76]

Introduction

Inhibition of aberrant signaling can inhibit tumor growth, and since the success of Gleevec as targeted therapy for chronic myeloid leukemia, the principle of specific targeting of aberrant signal transduction pathways by small-molecule inhibitors is thought to be a promising method to fight cancer (1, 2). This approach seems especially suitable for tumors with aberrations in upstream components of signaling cascades, cell surface receptors, or cytoplasmic kinases. Thus far, it has not been applied to tumors containing aberrations located at the end of signaling cascades, such as transcription factors, for which fewer, if any, specific small-molecule inhibitors are available. However, as transcription factors represent the second most frequently mutated class of proteins in tumors (3), the availability of specific inhibitory compounds against this class of proteins would broaden the principle of targeted therapy to many additional tumor types.

Rhabdomyosarcoma accounts for 5% to 8% of all pediatric malignancies and is the most common soft tissue sarcoma diagnosed in children (4). No targeted drug therapy is available for this tumor thus far. Histopathologically, rhabdomyosarcoma is subclassified into two major forms: alveolar rhabdomyosarcoma (aRMS) and embryonal rhabdomyosarcoma (eRMS). Eighty percent of the aRMS are characterized by specific translocations, involving the NH_2-terminal part of PAX3 or PAX7, which in the majority of cases is fused to the COOH-terminal part of FKHR generating chimeric transcription factors PAX3 (or PAX7)/FKHR. Overexpression of these translocation products is associated with a poor prognosis (5). Hence, the 5-year survival rate of aRMS patients is much lower compared with eRMS patients (6), and once metastasizing, aRMS become resistant to conventional chemotherapy and radiotherapy. Therefore, new therapeutic agents are urgently needed.

Survival of translocation-positive aRMS cells is dependent on continuous expression of the fusion protein, as down-regulation (7, 8) or inhibition by competition (9) of PAX3/FKHR induces apoptosis in aRMS cells. However, the technical complexity of their application *in vivo* prevents a clinical implementation of such methods up to now. Therefore, identification of other, clinically applicable, mechanisms for PAX3/FKHR inhibition would be of great interest.

In this study, we present evidence for a mechanism allowing regulation of PAX3/FKHR activity by the kinase inhibitor PKC412 (10). PKC412 is an inhibitor of several kinases, including protein kinase C (PKC), Akt/protein kinase B, c-Kit, FLT3, and fibroblast growth factor receptor (FGFR), and is being evaluated in phase II clinical trials for acute myelogenous leukemia (AML) patients (11). As we show here, the drug can influence the phosphorylation status of PAX3/FKHR and hence its transcriptional activity. Furthermore, we show a potent antitumorigenic potential of PKC412 for aRMS *in vitro* and *in vivo*. These studies suggest that controlling the activity of oncogenic transcription factors by small-molecule inhibitors is a promising therapeutic strategy against cancer.

Materials and Methods

Cell lines and pharmacologic inhibitors. Two aRMS cell lines (Rh4 and Rh30) and two eRMS cell lines (RD and Ruch-2) were used. The Rh4 cell line was obtained from the St. Jude Children's Hospital (Memphis, TN). The Rh30 and RD cell lines were purchased from the American Type Culture Collection (ATCC). The Ruch-2 cell line was established in our laboratories (12). For ectopic expression studies of PAX3/FKHR, 293T and NIH3T3 cells were used (ATCC).

PKI166, CGP59326, NVP-ABG424-NX-4, and PKC412 were provided by Novartis; rapamycin was purchased from Sigma.

3-(4,5-Dimethylthiazol-2-yl)-2,5-diphenyltetrazolium bromide assay. Twenty-four hours after seeding in 96-well plates, cells (10,000 per well) were treated with pharmacologic inhibitors in a volume of 100 μL medium including 10% serum for 96 h. 3-(4,5-Dimethylthiazol-2-yl)-2,5-diphenyltetrazolium bromide (MTT) assays (Roche) were then performed according to the manufacturer's protocol.

Note: R. Amstutz and M. Wachtel contributed equally to this work.

Requests for reprints: Beat W. Schäfer, Department of Oncology, University Children's Hospital, Steinwiesstrasse 75, CH-8032 Zurich, Switzerland. Phone: 41-44-266-75-53; Fax: 41-44-266-71-71; E-mail: beat.schaefer@kispi.uzh.ch.

doi:10.1158/0008-5472.CAN-07-2447

Trypan blue exclusion assay. Cells (10^6) were seeded in 10-cm dishes and, 24 h later, incubated with pharmacologic inhibitors for 96 h. Floating and adherent cells were then pooled, spun down, and resuspended in a defined volume of medium. After diluting the cells 1:1 with 0.4% of trypan blue solution (Sigma), alive and dead cells were counted.

Caspase-3 assay. Active caspase-3 was detected by the CaspGLOW Red Active Caspase-3 Staining kit (BioVision) according to the manufacturer's instructions. Briefly, 3×10^5 cells per six-well plate were treated with 0.5 μmol/L PKC412 for 24 to 72 h, and then floating and trypsinized cells were pooled, spun down, and incubated with Red-DEVD-FMK caspase-3 inhibitor for 45 min at 37°C. Cells positive for active caspase-3 were scored by fluorescence microscopy.

Immunoblotting. Immunoblotting was performed as described previously (13) using primary antibodies against poly(ADP-ribose) polymerase (PARP; 1:1,000; Cell Signaling Technology), FKHR (C20; 1:500; Santa Cruz Biotechnology), proliferating cell nuclear antigen (1:1,000; BD Transduction Laboratories), actin (A2103; 1:1,000; Sigma), and Tetra-His (1:1,000; Qiagen).

Immunofluorescence. Immunofluorescence of cells plated on gelatin-coated glass coverslips was performed as described previously (13) using a primary antibody against Tetra-His (1:200) and an Alexa Fluor 488–labeled secondary antibody (1:200; Invitrogen, Molecular Probes).

Purification of the PAX3 DNA-binding domain protein. The PAX3 part represented in the translocation product PAX3/FKHR (AA1-391 of PAX3) was His tagged (NterPAX3His) and transiently expressed in 293T cells. Forty-eight hours after transfection, the cells were lysed in a buffer containing 50 mmol/L NaH_2PO_4 (pH 8.0), 1% Triton X-100, 300 mmol/L NaCl, 10 mmol/L imidazole, 40 mmol/L NaF, 10 mmol/L β-glycerolphosphate, 1 mmol/L Na_3VO_4, 1 mmol/L EGTA, and 1× complete protease inhibitor mix including 1 mmol/L EDTA (Roche). After centrifugation of the extract at 10,000 × *g* for 10 min, the supernatant was incubated with 8 μL/mL 50% Ni-NTA agarose (Qiagen) for 2 h at 4°C. The Ni-NTA agarose was then washed four times with a buffer containing 50 mmol/L NaH_2PO_4 (pH 8.0), 300 mmol/L NaCl, and 20 mmol/L imidazole and two times with a similar washing buffer containing 50 mmol/L imidazole. The protein was eluted with a similar buffer containing 250 mmol/L imidazole.

For some applications, the protein was desalted using a C8 reversed-phase high-performance liquid chromatography (HPLC) column (Brownlee Aquapore RP-300, 2.1 × 100 mm; Perkin-Elmer).

Two-dimensional SDS-PAGE. Isoelectric focusing was performed on an IPGphor electrophoresis unit (Amersham Pharmacia Biotech) according to standard protocols (14). Immobiline IPG strips with a nonlinear pH gradient of 3 to 10 (Amersham) were used and the samples were applied on the strips by in-gel rehydration. SDS-PAGE was carried out on a Protean II xi system (Bio-Rad) with 40 mA/gel at 15°C. Gels consisted of 13% (w/v) acrylamide with 2.7% piperazine diacrylamide as cross-linker. Proteins were visualized by a long silver nitrate staining.

Enzymatic digestion and liquid chromatography matrix-assisted laser desorption/ionization time-of-flight mass spectrometry analysis of the peptides. The desalted protein solution was dried in a vacuum centrifuge and redissolved in a solution containing 150 mmol/L Tris, 6 mol/L urea, and 6 mmol/L EDTA (pH 8). Ten microliters were then incubated for 2 h at 37°C. Five microliters of a solution containing 0.5 μg of Lys C (Roche Diagnostics) and 45 μL H_2O were added and incubated overnight at 37°C.

Peptides were separated on a reversed-phase capillary HPLC column (PepMap C18, 0.3 × 150 mm; LC Packings) and collected onto a 600-μm AnchorChip target (Bruker Daltonics), using a Probot microfraction collector (LC Packings), in 15-s intervals. Matrix solution (1.5 μL) was added to each fraction. A 1:10 dilution of saturated HCCA (α-cyano-4-hydroxycinnamic acid in 33% CH_3CN, 0.1% trifluoroacetic acid) in ethanol/acetone 2:1 was used as matrix solution. Mass mapping was performed with an Autoflex matrix-assisted laser desorption/ionization time-of-flight mass spectrometry (MALDI-TOF-MS; Bruker Daltonics). Phosphorylated peptides were analyzed in the linear positive ion mode with delayed extraction (60 ns), and the following voltages were applied: source, 20 kV; extraction, 18.80 kV; lens, 7.85 kV.

Protein analysis with liquid chromatography-electrospray ionization MS. Electrospray ionization MS (ESI-MS) was performed on a PE SCIEX API 365 liquid chromatography (LC)-MS/MS system. Mass spectra were acquired in the mass range of *m/z* 1,000 to 3,000 with step size of 0.1 (scan time, 6 s). Chromatographic separation was performed on an Ultimate system (LC Packings) equipped with a Vydac C8 capillary column (0.3 × 150 mm). The flow rate was 4 μL/min.

***In vivo* labeling with [^{32}P]orthophosphate.** 293T cells were transfected with NterPAX3His or empty vector. Thirty-six hours after transfection, cells were washed twice with phosphate-free MEM and then incubated for 6 h in phosphate-free MEM supplemented with 80 μCi/mL [^{32}P]orthophosphate (GE Healthcare, Amersham). Thereafter, NterPAX3His was purified with the help of Ni-NTA agarose. Purified proteins were Western blotted followed by detection of ^{32}P with a phosphorimager (Molecular Dynamics).

Transactivation assay. PAX3/FKHR or PAX3 constructs together with a reporter plasmid containing the *luciferase* gene downstream of PAX3 paired domain or homeodomain DNA-binding sites [6×CD19 DNA-binding sites (15) or P3-binding site (16)] and a plasmid containing the *lacZ* gene were transfected into 293T or NIH3T3 cells or electroporated into Rh4 cells using the AMAXA system (Program O17, buffer R) in ratios ensuring measurement in the linear range of the assay. Similarly, a FKHR construct together with a reporter plasmid containing the *luciferase* gene downstream of the bim promoter (17) and a plasmid containing the *lacZ* gene was transfected into NIH3T3 cells.

For measurement of effects of PKC412, cells were incubated 16 h after transfection with PKC412 or DMSO vehicle for 24 h followed by lysis in reporter lysis buffer (Promega). β-Galactosidase and luciferase activities were determined with the corresponding assay systems (Promega). Luciferase activity values were normalized with the β-galactosidase activity values and values of empty vector controls were subtracted.

Mutagenesis. PAX3/FKHR mutants were generated using the GeneTailor Site-Directed Mutagenesis System (Invitrogen) according to the manufacturer's instructions. All constructs were sequenced for verification.

Silencing of PAX3/FKHR. Silencing of PAX3/FKHR by small interfering RNA (siRNA) was performed as described previously (8).

Real-time PCR. Quantitative reverse transcription-PCR (qRT-PCR) was performed under universal cycling variables on an ABI 7900 instrument using commercially available target probes and Mastermix (all from Applied Biosystems, Applera Europe BV). Detection of PAX3/FKHR was achieved using PAX3 forward (5′-GCACTGTACACCAAAGCACG-3′) and FKHR reverse (5′-AACTGTGATCCAGGGCTGTC-3′) primers applying the fluorescent SYBR green method (Applied Biosystems). Cycle threshold (C_T) values were normalized to glyceraldehyde-3-phosphate dehydrogenase (GAPDH). Relative expression levels of the target genes among the different samples were calculated using the $\Delta\Delta C_T$ method.

CIP treatment of NterPAX3His. Twelve microliters of purified NterPAX3His or nuclear extracts of 293T cells overexpressing NterPAX3His were incubated with calf intestinal phosphatase (CIP) buffer alone, 10 units CIP (Promega), or 10 units of CIP in the presence of 60 mmol/L EDTA and 4 mmol/L Na_3VO_4 as phosphatase inhibitors in a volume of 20 μL for 30 min at 37°C. Reactions without inhibitors were stopped by adding 60 mmol/L EDTA and 4 mmol/L Na_3VO_4.

Electrophoretic mobility shift assay. Electrophoretic mobility shift assay (EMSA) with biotinylated oligonucleotides containing a homeodomain-binding site (5′-TGATTGCGGTGCTAATTGATTAACTTCG-CATACCTGAT-3′) or a paired domain–binding site (5′-CTGGAGGGTTCC-TGGAGAATGGGGCCTGAGGCGTGACCACCGCCTTCCTCTCTGGG-3′) was performed as described previously (15). EMSA reactions were resolved in 6% DNA retardation gels (Invitrogen) followed by blotting onto nylon membranes (Millipore). Oligos were detected using the chemiluminescent nucleic acid detection module (Pierce).

Rhabdomyosarcoma xenograft studies. Rh4 or Rh30 cells (10^7) were injected into the right flank of athymic CD1 nude (*nu/nu*) mice (Charles River). When tumors reached a volume of 130 to 200 mm^3, oral treatment with PKC412 (100 mg/kg/d) or placebo for 15 d was started. Tumor diameters (d_1, d_2) were measured thrice weekly using a digital caliper. Tumor volumes were calculated with the following formula: $V = (4/3)\pi r^3$,

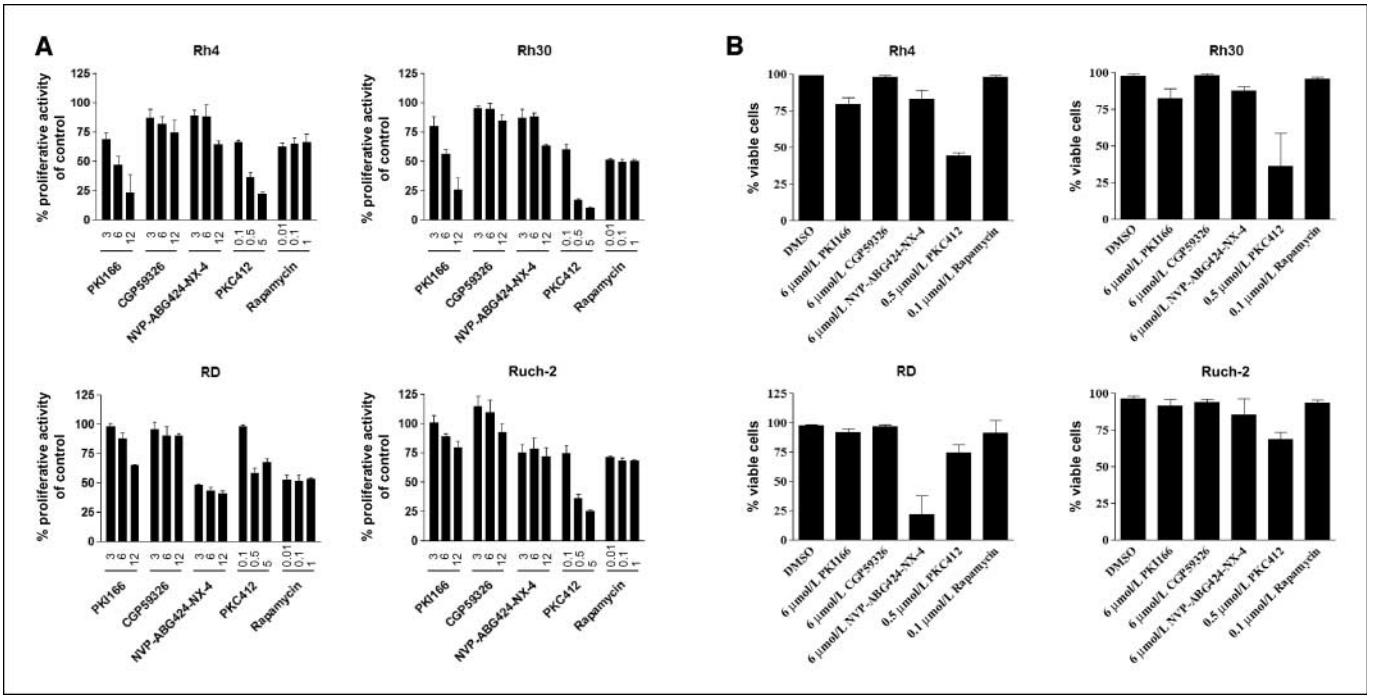

Figure 1. Screening of small-molecule inhibitors for growth-inhibitory effects on aRMS (Rh4 and Rh30) and eRMS (RD and Ruch-2) cell lines. *A,* changes in proliferative activity as measured by MTT assays. Inhibitors were applied for 96 h at three concentrations (indicated in μmol/L). *Columns,* mean of three independent experiments each performed in triplicate; *bars,* SD. *B,* cell death was assessed using trypan blue exclusion. Cells were treated with the median concentration of the inhibitors described in *A* for 96 h. *Columns,* mean of three independent experiments; *bars,* SD.

where $r = [(d_1 + d_2) / 4]$. At the end of the treatment period, tumors were isolated and fixed in 4% paraformaldehyde in PBS. Cell proliferation was assessed by Ki-67 immunostainings (clone SP6; NeoMarkers). Furthermore, apoptosis was detected by terminal deoxynucleotidyl transferase–mediated dUTP nick end labeling (TUNEL) staining according to the manufacturer's instructions (*In Situ* Cell Death Detection Kit, Fluorescin, Roche). Ki-67–positive or TUNEL-positive cells were scored in 10 randomly selected visual fields.

Results

Treatment of rhabdomyosarcoma cells with kinase inhibitors. Recent gene expression studies of rhabdomyosarcoma (18) identified a series of receptor tyrosine kinases (RTK) with potential oncogenic capabilities highly expressed in rhabdomyosarcoma. Therefore, we tested a series of small-molecule inhibitors targeting RTKs in comparison with the mammalian target of rapamycin (mTOR) inhibitor rapamycin (19) for potential growth-inhibitory effects on two aRMS (Rh4 and Rh30) and two eRMS (RD and Ruch-2) cell lines, as assessed by MTT assay (Fig. 1*A*). Induction of cell death by the different inhibitors was measured by trypan blue exclusion assays (Fig. 1*B*).

In accordance with previous studies (19), rapamycin showed growth-inhibitory effects for both aRMS and eRMS cells (Fig. 1*A*). However, the effects for Rh4 and Ruch-2 cells were small and no clear dose-response relationship was found within the tested concentration range. Furthermore, no significant loss of cell viability was observed (Fig. 1*B*).

PKI166 and CGP59326, known to block the activity of either both epidermal growth factor receptor (EGFR; ErbB1) and ErbB2 or only EGFR, respectively, affected neither cell growth nor viability (CGP59326) or inhibited cell growth but without significant induction of cell death (PKI166; Fig. 1*A* and *B*), suggesting inhibition of proliferation rather than induction of cell death in rhabdomyosarcoma cell lines.

The c-met inhibitor NVP-ABG424-NX-4 influenced cell growth in all rhabdomyosarcoma cell lines moderately, except for RD cells (Fig. 1*A*), in which a dramatic induction of cell death was observed, suggesting that strong sensitivity to this drug was observed in one cell line only.

Finally, PKC412 inhibited proliferation of the aRMS cells Rh4 and Rh30 much more effectively than RD and Ruch-2 cells (Fig. 1*A*). In addition, cell death was significantly induced only in aRMS and not in eRMS cells (Fig. 1*B*).

Taken together, among the inhibitors tested, PKC412 showed the most efficient and specific antiproliferative effect for aRMS cells. Therefore, PKC412 was further characterized.

Therapeutically significant IC_{50} levels for PKC412 were only achieved in aRMS cells (Fig. 2*A*). To investigate whether cell death is due to apoptosis, we used an activated caspase-3 assay. As shown in Fig. 2*B*, induction of caspase-3–dependent apoptosis dramatically increased in aRMS cells when treated with 0.5 μmol/L PKC412 for 24 to 72 h. In contrast, apoptosis was only marginally enhanced in eRMS cells. This finding was confirmed by examining the caspase-3 substrate PARP (Fig. 2*C*), which was cleaved as early as 4 h after incubation with 0.5 μmol/L PKC412 (Fig. 2*B*). Therefore, PKC412 selectively induces caspase-3–dependent apoptosis in aRMS but not in eRMS cells.

PKC412 influences the transcriptional activity of PAX3/FKHR. aRMS cells are known to undergo apoptosis on silencing of PAX3/FKHR by oligonucleotides (7) or siRNA (8).

Hence, we hypothesized that PKC412 might influence PAX3/FKHR activity. In the absence of PKC412, ectopic expression of PAX3/FKHR in 293T cells induces transcription of CB1, as detected by qRT-PCR (Fig. 3*A*). A mutation (N269A) within the

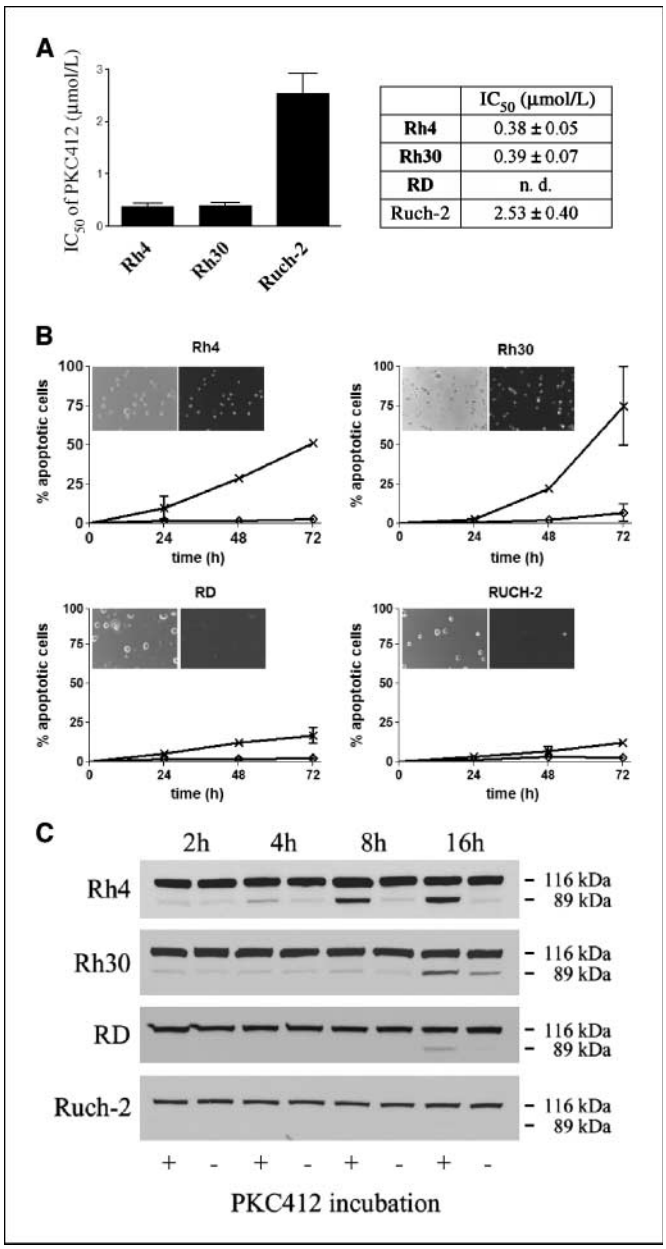

Figure 2. PKC412 induces apoptosis in aRMS but not in eRMS cell lines. *A,* IC_{50} values of PKC412 as determined by MTT assays of rhabdomyosarcoma cells treated with increasing concentrations of PKC412 (0–10 μmol/L) for 96 h. Note that the IC_{50} value for RD cells was not determinable (*n.d.*) because a 50% inhibition of proliferative activity could not be achieved. *Columns,* mean of three independent experiments performed in triplicate; *bars,* SD. *B,* identification of apoptotic cells by an activated caspase-3 assay after treatment with 0.5 μmol/L PKC412 (×) or DMSO (◇) for 24 to 72 h. *Points,* mean of three independent experiments; *bars,* SD. Corresponding phase-contrast and fluorescence images display total and apoptotic cells after 72 h, respectively. *C,* Western blot analysis of PARP cleavage in rhabdomyosarcoma cells after treatment with 0.5 μmol/L PKC412 or DMSO for 2, 4, 8, and 16 h.

homeodomain of PAX3, specifically inactivating its homeodomain DNA binding (16), prevents induction of CB1 transcription (Fig. 3*A*) but not of the paired domain–dependent target gene *AP2β* (data not shown; ref. 8). This strongly suggests that activation of CB1 transcription in 293T cells is dependent on PAX3/FKHR activity, confirming results of earlier studies (20). Furthermore, specific silencing of PAX3/FKHR by siRNA in Rh4 cells reduced CB1 expression to <20% compared with control (Fig. 3*A*). The transcriptional level of CB1 was therefore used to monitor PAX3/FKHR activity in further experiments.

Surprisingly, in the presence of PKC412, PAX3/FKHR-induced transcription of CB1 in 293T cells as well as endogenous mRNA levels in Rh4 cells were inhibited (Fig. 3*B*). This inhibitory effect of PKC412 was validated by transactivation assays using luciferase reporter plasmids containing specific promoters for the paired domain (6×CD19) or the homeodomain (P3) of PAX3. In these assays, PKC412 strongly reduced PAX3/FKHR-induced expression of the reporter in both 293T and Rh4 cells (Fig. 3*B*).

To exclude that PKC412 mediates these effects via down-regulation of PAX3/FKHR expression, mRNA and protein levels were measured in transfected 293T and Rh4 cells. Surprisingly, PKC412 incubation led to an increase of PAX3/FKHR on the mRNA as well as on the protein level in 293T cells, whereas in Rh4 cells PAX3/FKHR levels were only slightly influenced (Fig. 3*C*). Taken together, these results suggest that PKC412 modulates the transcriptional activity of PAX3/FKHR.

To evaluate which part of the fusion protein is target of this PKC412 effect, we measured its influence on the activity of the translocation product PAX3/NCOA1 (18) and on PAX3 and FKHR alone. This approach showed that PKC412 inhibited induction of CB1 by PAX3/NCOA1 as well as the transactivation activity of PAX3 very similar to PAX3/FKHR (Fig. 3*D*). In contrast, the transactivation potency of FKHR on a luciferase reporter driven by the promoter of the FKHR target gene *bim* (17) was unchanged by PKC412 (Fig. 3*D*). Taken together, these data suggest that it is the PAX3 rather than the FKHR domain of the fusion protein that is influenced by PKC412.

The PAX3 domain of PAX3/FKHR is phosphorylated at multiple sites. We hypothesized that the kinase inhibitor PKC412 might affect potential phosphorylation sites within the PAX3 domain as a mechanism to reduce activity. We therefore searched for phosphorylations within this domain directly using a His-tagged form (NterPAX3His). Immunofluorescence of transfected 293T cells with an anti-His tag antibody confirmed that NterPAX3His was localized in the nucleus, as known for full-length PAX3/FKHR (Fig. 4*A*), which was not changed after incubation with 10 μmol/L PKC412 for 24 h. NterPAX3His was then purified from ^{32}P-labeled 293T cells and tested for potential phosphorylation. As shown in Fig. 4*B*, a strong ^{32}P signal was detected in the NterPAX3His protein, showing that PAX3 is indeed a phosphoprotein. Analysis with two-dimensional gel electrophoresis further supported this conclusion, as the purified NterPAX3His protein appeared as mixture of several species with different isoelectric points (pI), reminiscent of multiple phosphorylation sites in the protein (Fig. 4*B*). Treatment of purified NterPAX3His protein or nuclear extracts from 293T cells overexpressing NterPAX3His with CIP reduced the ability of NterPAX3His to bind to oligonucleotides containing a homeodomain-specific or a paired domain–specific binding site (Fig. 4*C*), suggesting that phosphorylation influences DNA-binding properties of PAX3.

LC-MALDI-TOF-MS analysis of Lys C–digested PAX3-His protein revealed four (or probably five) phosphates in the peptide 186 to 216 (Fig. 4*D*). This peptide contains six serine residues (S187, S193, S197, S201, S205, and S209) as potential phosphorylation sites (Fig. 4*D*). Four of these six serine residues are conserved among the PAX3 proteins from different species, suggesting irreplaceability for proper function of PAX3 (Fig. 4*D*). Interestingly, *in silico* analysis using different web resources revealed that these six serine residues

and the two flanking S180 and S222 have the highest probability for being phosphorylated in PAX3 (data not shown).

Phosphorylation influences activity of PAX3/FKHR. To test directly whether PKC412 influences the phosphorylation status of NterPAX3His, protein purified from PKC412- and control-treated 293T cells was analyzed by two-dimensional gel electrophoresis. As shown in Fig. 5*A*, PKC412 induced a clear shift toward more basic pIs. Furthermore, ESI-MS (Fig. 5*A*) as well as MALDI-TOF-MS (data not shown) analysis of the same proteins revealed a PKC412 treatment–induced shift toward smaller protein species. These

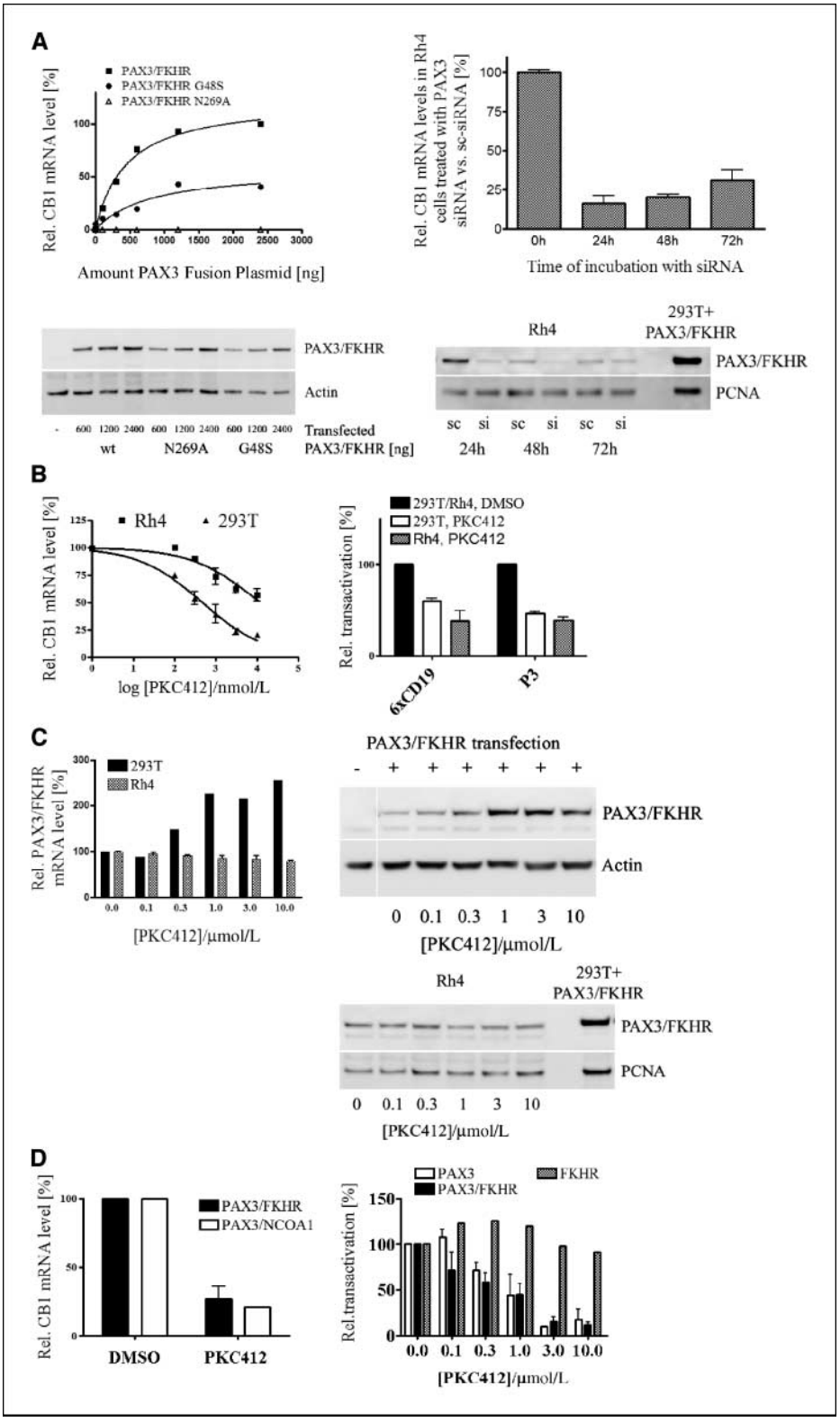

Figure 3. PKC412 inhibits the transcriptional activity of PAX3/FKHR and PAX3. *A, top left,* induction of transcription of the PAX3/FKHR target gene *CB1* in 293T cells on ectopic expression of the indicated PAX3/FKHR constructs as measured by qRT-PCR. Results of one representative experiment are shown. *Bottom left,* levels of PAX3/FKHR wt and mutant protein in 293T cells transfected with the indicated amount of PAX3/FKHR plasmid as detected by Western blot with an anti-FKHR antibody. Actin, loading control. *Top right,* effect of siRNA-mediated silencing of PAX3/FKHR on the transcription level of CB1 in Rh4 cells as measured by qRT-PCR at the indicated time points. CB1 mRNA levels were normalized with GAPDH levels. *Bottom right,* levels of PAX3/FKHR protein in Rh4 cells on treatment with anti-PAX3 (*si*) or scrambled (*sc*) siRNA for the indicated times. PCNA, loading control. *B, left,* effect of PKC412 on ectopic PAX3/FKHR-induced CB1 transcription in 293T cells and on endogenous CB1 transcription in Rh4 cells as measured by qRT-PCR. Cells were incubated with the indicated concentration of PKC412 for 16 h. *Points,* mean of three independent experiments; *bars,* SD. *Right,* relative luciferase levels after transfection of PAX3/FKHR and reporters with specific promoters for the paired domain (*6×CD19*) or the homeodomain (*P3*). Rh4 or 293T cells transfected with PAX3/FKHR were incubated with 10 μmol/L PKC412 for 16 h. *Columns,* mean of three independent experiments; *bars,* SD. *C, left,* PAX3/FKHR mRNA levels in transfected 293T and Rh4 cells measured by qRT-PCR. Cells were treated as described in *B. Right,* PAX3/FKHR protein levels in transfected 293T cells (*top*) or Rh4 cells (*bottom*) measured by Western blot detection with an anti-FKHR antibody. Cells were treated as described in *B.* Actin and PCNA, loading controls. *D, left,* transcriptional activation of CB1 by PAX3/FKHR and PAX3/NCOA1. 293T cells were transfected with the indicated PAX3 fusion protein construct and incubated with 10 μmol/L PKC412 for 16 h. *Right,* transactivation potency of PAX3, PAX3/FKHR, and FKHR. NIH3T3 cells transfected with PAX3 or PAX3/FKHR together with the 6×CD19 reporter plasmid or FKHR together with the bim reporter plasmid were incubated with the indicated concentrations of PKC412 for 16 h before measurement of reporter expression. *Columns,* mean of three independent experiments; *bars,* SD.

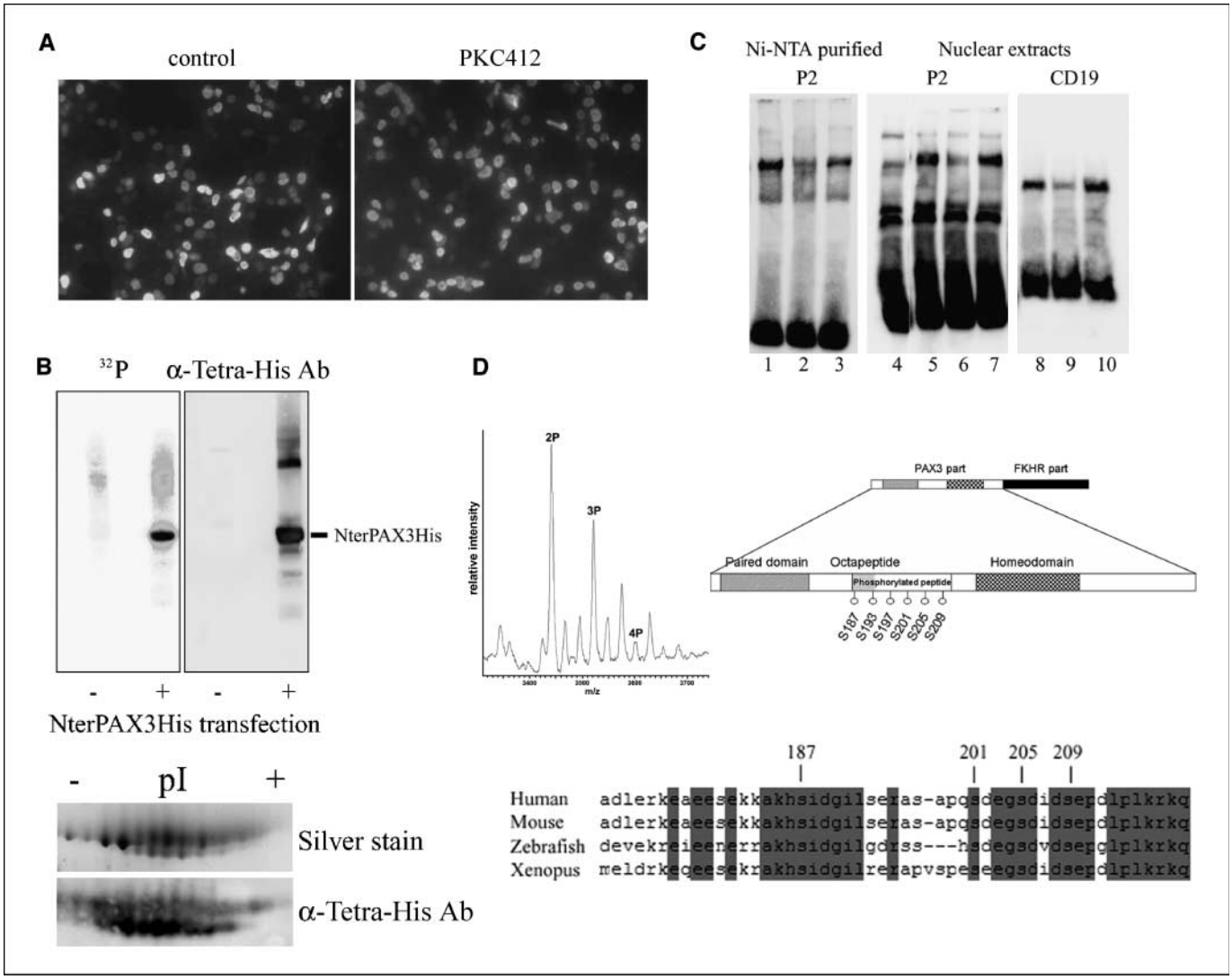

Figure 4. The PAX3 part of PAX3/FKHR is phosphorylated *in vivo. A,* immunofluorescent detection of NterPAX3His with an α-Tetra-His antibody in transfected 293T cells cultivated in the presence or absence of 10 μmol/L PKC412 for 24 h. *B, top,* phosphorimager detection of ^{32}P (*left*) and α-Tetra-His immunodetection (*right*) of Western blotted NterPAX3His protein purified from ^{32}P-labeled 293T cells ectopically expressing NterPAX3His (*right lanes*). *Left lanes,* mock-transfected cells were processed as control. *Bottom,* silver-stained two-dimensional gel of NterPAX3His protein purified from 293T cells (*upper*) and α-Tetra-His immunodetection of a blotted two-dimensional gel of the same protein (*lower*). *C,* EMSA of purified NterPAX3His protein (*lanes 1–3*) and nuclear extract of control-transfected (*lane 4*) or NterPAX3His-transfected (*lanes 5–10*) 293T cells with oligos containing a homeodomain-binding (*lanes 1–7*) or a paired domain–binding (*lanes 8–10*) site. Protein samples used for EMSA were preincubated with CIP buffer alone (*lanes 1, 5*, and *8*), CIP (*lanes 2, 6*, and *9*), or CIP in the presence of phosphatase inhibitors (*lanes 3, 7*, and *10*), respectively. *D, top left,* MALDI-TOF mass spectrum of the peptide 186 to 216 of PAX3. NterPAX3His was purified from NterPAX3His-transfected 293T cells and digested by Lys C. Resulting peptides were isolated by chromatography and investigated for phosphorylation by MALDI-TOF-MS. 2P, 3P, and 4P assign peaks of the 2-, 3-, and 4-fold phosphorylated peptide, respectively. *Top right,* schematic representation of the domain structure of PAX3 depicting the localization of the identified phosphorylation sites in PAX3. *Bottom,* alignment of the PAX3 protein sequences from the indicated species in the region with identified phosphorylation sites. Potential phosphorylation sites conserved among all four species (S187, S201, S205, and S209) are indicated.

results suggest that PKC412 affects the posttranslational modification of PAX3.

To test whether phosphorylation directly affects PAX3/FKHR activity, we mutated the six serine residues individually into aspartate to mimic phosphorylation. However, these single mutations did not affect sensitivity of PAX3/FKHR toward PKC412 (data not shown). Instead, mutation of all six serine residues together into aspartate (PAX3/FKHR 6×D) rescued, at least partially, transcriptional activity of PAX3/FKHR (Fig. 5*B, left*). As expressed protein levels of wild-type (wt) and mutated protein were similar (Fig. 5*B, right*), this suggests involvement of more than one of these sites in regulation of PAX3/FKHR activity. Additional mutation of S180 into aspartate (PAX3/FKHR 7×D) did not lead to a significant further increase in rescue (Fig. 5*B*), whereas mutation of S222 led to complete loss of transactivation activity (data not shown). In accordance with the behavior of the aspartate mutants, also single loss-of-function mutations of the six serine residues into alanine did not affect transactivation potencies (data not shown), whereas multiple mutations decreased transactivation activity as measured in transactivation assays using the 6×CD19 reporter plasmid up to ~50% (Fig. 5*C*).

To test whether these phosphorylation sites are involved in regulation of PAX3 DNA binding, we treated nuclear extracts of 293T cells transfected with wt NterPAX3His or NterPAX3His 7×D with CIP. EMSA experiments showed that, in contrast to wt NterPAX3His, DNA binding of the mutant NterPAX3His 7×D to

both paired domain–specific or homeodomain-specific oligos was not influenced by CIP treatment (Fig. 5*D, left*). This suggests that indeed phosphorylation influences DNA binding of NterPAX3His. To test whether also PKC412 affects DNA binding of PAX3/FKHR, EMSA was performed with nuclear extracts from PAX3/FKHR-transfected cells incubated with or without 10 μmol/L PKC412. As shown in Fig. 5*D* (*right*), PKC412 treatment indeed decreases DNA binding of PAX3/FKHR.

Taken together, we conclude that specific phosphorylation positively influences DNA binding of PAX3, thereby modulating PAX3(/FKHR) activity, which in turn can be influenced by PKC412 treatment.

Inhibition of *in vivo* tumor growth of aRMS xenografts by PKC412. As kinase inhibitors are interesting molecules for potential treatment of aRMS, we further investigated the effects of PKC412 on tumor growth *in vivo*. Toward this end, Rh4 and Rh30 xenograft mice were treated daily by oral administration of PKC412 (100 mg/kg) for 15 days. In both xenograft models, tumor growth was significantly inhibited by PKC412 (Fig. 6*A*). In Rh4 xenografts, a complete suppression of tumor growth was observed, whereas in Rh30 xenografts tumor growth was strongly decreased.

To further characterize the effect of PKC412 on xenografts, the tumors were isolated and characterized. Tumor morphology was determined by H&E stainings. Placebo-treated Rh4 and Rh30 xenograft sections (Fig. 6*C, top row*) both showed a high density of actively growing tumor cells. In contrast, PKC412-treated tumors showed a dramatic increase in extracellular material (Rh4 xenografts; Fig. 6*C, bottom left*) and/or necrotic areas (Rh30 xenografts; Fig. 6*C, bottom right*).

To quantify the influence of PKC412 on tumor cell proliferation *in vivo*, tumor sections were immunohistochemically stained for the proliferation marker Ki-67 and apoptotic cells were detected by TUNEL staining. As shown in Fig. 6*B*, the number of Ki-67–positive cells was decreased in both Rh4 and Rh30 xenografts after treatment, whereas the number of apoptotic tumor cells was dramatically increased by 4- to 5-fold in tumors isolated from both Rh4 and Rh30 xenograft mice treated with PKC412.

In summary, PKC412 significantly inhibited tumor growth and reduced numbers of actively dividing tumor cells while simultaneously increasing number of apoptotic cells *in vivo*.

Discussion

For rhabdomyosarcoma, the current treatment is still based on conventional treatment regimens (surgery, chemotherapy, and radiotherapy), which in the case of metastasized aRMS often fail. Alternative treatment agents are therefore highly desired.

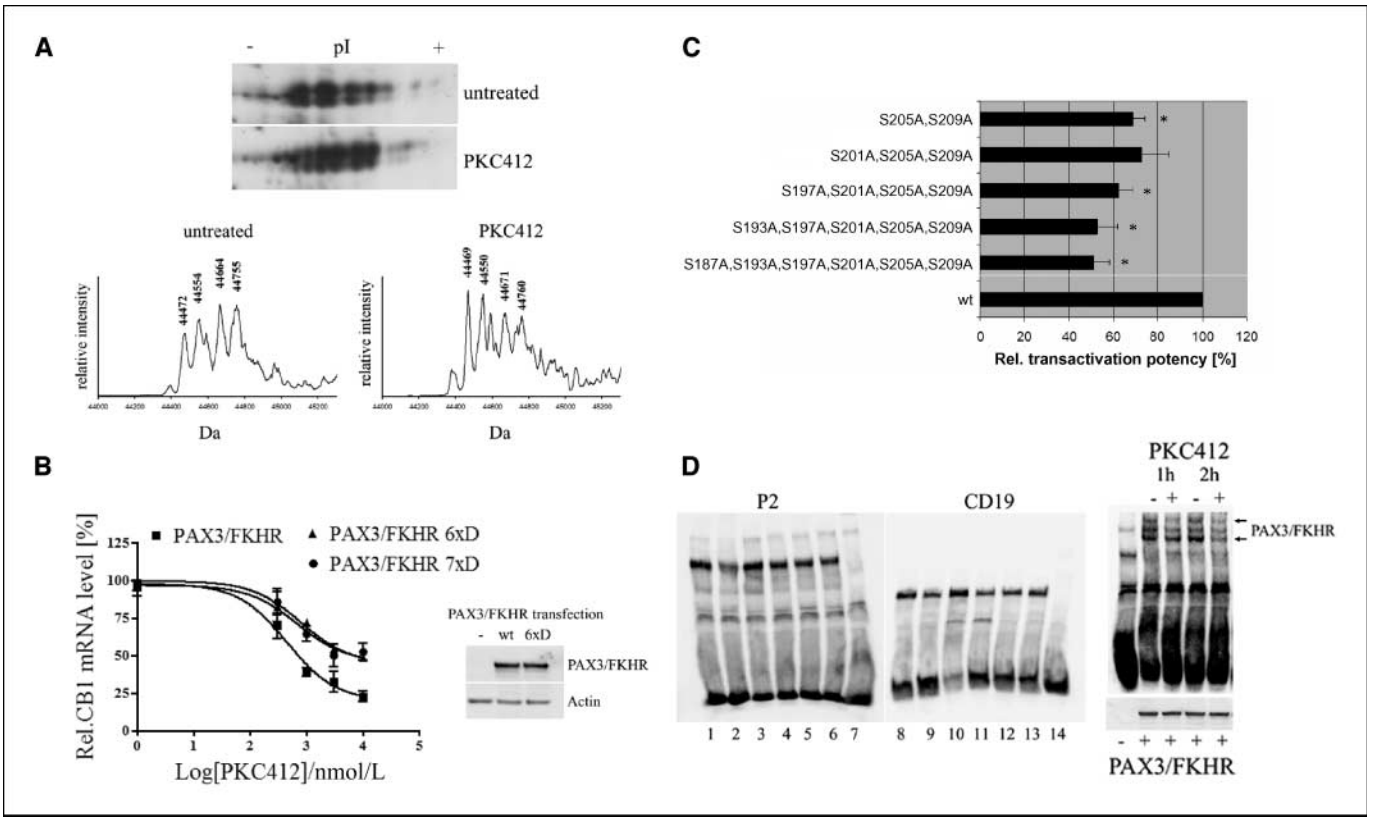

Figure 5. PKC412 influences phosphorylation of PAX3/FKHR. *A, top,* silver-stained two-dimensional gel of NterPAX3His protein purified from transfected 293T cells untreated (*upper*) or treated with 10 μmol/L PKC412 (*lower*) for 16 h. *Bottom,* ESI-MS analysis of the same proteins as in *A. B, left,* effect of PKC412 on induction of CB1 transcription in 293T cells on ectopic expression of wt or mutant PAX3/FKHR as measured by qRT-PCR. *Points,* mean of three independent experiments; *bars,* SD. *Right,* expression levels of the indicated PAX3/FKHR forms on transfection into 293T cells. Actin, loading control. *C,* relative transactivation potencies of wt PAX3/FKHR or PAX3/FKHR with the indicated serine-alanine mutations on the 6×CD19 reporter plasmid as measured by luciferase assays. *Columns,* mean of three independent experiments; *bars,* SD. *, $P < 0.05$, compared with wt. *D, left,* EMSA with nuclear extracts of 293T cells transfected with NterPAX3His wt (*lanes 1–3* and *8–10*) or with NterPAX3His 7×D (*lanes 4–6* and *11–13*) and of untransfected cells (*lanes 7* and *14*). Nuclear extracts were either incubated with CIP buffer alone (*lanes 1, 4, 8*, and *11*), treated with CIP (*lanes 2, 5, 9*, and *12*), or treated with CIP in the presence of phosphatase inhibitors (*lanes 3, 6, 10*, and *13*). EMSAs were performed with homeodomain-specific (*P2*) or paired domain–specific (*CD19*) oligos. *Right, top,* EMSA with nuclear extracts from untransfected (*left lane*) or PAX3/FKHR-transfected (*right four lanes*) 293T cells and the homeodomain-specific oligo. Cells were incubated with 10 μmol/L PKC412 or vehicle alone for 1 and 2 h as indicated. *Bottom,* expression levels of PAX3/FKHR in the nuclear extracts used for EMSA as detected by an anti-FKHR antibody.

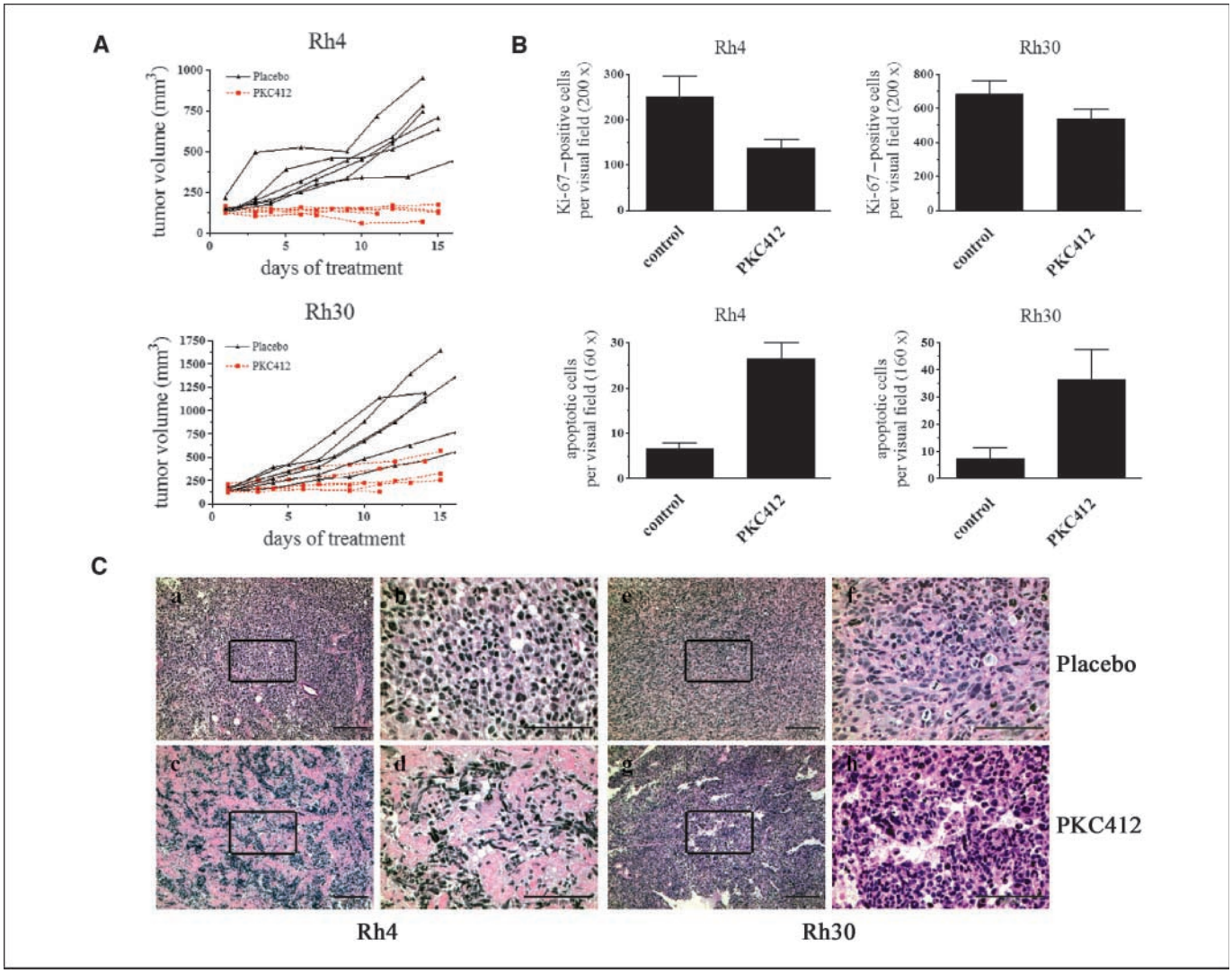

Figure 6. *In vivo* antitumor effects of PKC412 in two different aRMS xenograft models. *A,* growth inhibition of Rh4 and Rh30 xenografts in female CD-1 athymic nude mice (*nu/nu*) treated with a daily dose of 100 mg/kg PKC412 for up to 15 d. *B,* evaluation of proliferation and apoptosis in PKC412-treated xenografts by immunohistochemistry and TUNEL staining. Tumor sections were stained for Ki-67 (*top row*) or TUNEL-stained (*bottom row*). Proliferation and apoptosis were quantified by counting Ki-67–positive and TUNEL-positive cells. *Columns,* mean of each treatment group ($n = 3$–6); *bars,* SD. *C,* H&E stainings of Rh4 (*a–d*) and Rh30 (*e–h*) xenograft sections. *Top row,* placebo-treated tumors; *bottom row,* PKC412-treated tumors. Cells within the square in left panels are shown in right panels at higher magnification. *Bars,* 200 μm (*left*) and 100 μm (*right*).

In an approach to find targetable pathways in rhabdomyosarcoma, we analyzed recent gene expression data of rhabdomyosarcoma biopsies (18) for the expression of kinases with a known tumor relation and tested a series of kinase inhibitors against three selected kinases (EGFR, hepatocyte growth factor receptor, and FGFR) in comparison with mTOR, which has been characterized as target in rhabdomyosarcoma *in vitro* (19), for their ability to specifically reduce the growth of different aRMS and eRMS cell lines.

From all substances tested, PKC412 was found to have the most promising antigrowth effect with specificity against the aRMS subgroup. This compound induces very efficient apoptosis in submicromolar concentrations, which is well below the steady-state plasma levels of 2 to 7 μmol/L, which were achieved in phase I clinical trials with this substance (21). As these concentrations were well tolerated by patients, our *in vitro* data provide a first preclinical rationale for clinical studies of aRMS treatment.

PKC412 is a derivative of staurosporine and was developed as PKC inhibitor. Although being more specific when compared with staurosporine, which is known to bind to a bulk of the whole kinome (22), PKC412 was found to inhibit a wide range of kinases, such as cyclin-dependent kinase 1/cyclin B, protein kinase A, c-src, and KDR (vascular endothelial growth factor receptor 2), in submicromolar concentrations (23). Based on these characteristics, PKC412 has been successfully applied as inhibitor of different oncogenic kinases in a range of tumors *in vitro* [e.g., as FGFR inhibitor in myeloproliferative disorder or multiple myeloma (24, 25), as Kit inhibitor in mast cell leukemia (26), or as Akt inhibitor in myeloma (27)]. Its potential clinical use is most advanced as FLT3 inhibitor for the treatment of AML, for which PKC412 is used in a phase II clinical study (11).

Mechanistically, we found an unexpected inhibitory effect of PKC412 on transcriptional activity of PAX3/FKHR, an important potential therapeutic target in rhabdomyosarcoma. This effect is

based on several observations: induction of target gene transcription on ectopic expression in the nonrhabdomyosarcoma cell line 293T can be inhibited. In addition, in the aRMS cell line Rh4, the endogenous transcription of these target genes is affected by PKC412, albeit less pronounced. However, whereas 293T cells do tolerate even 10 μmol/L PKC412, aRMS cells rapidly undergo apoptosis on PKC412 treatment, thereby interfering with determination of target gene levels. In contrast, when using reporter plasmid–based transactivation systems to measure PAX3/FKHR activity, the effects of PKC412 in both 293T and Rh4 cells were comparable, suggesting effective inhibition of PAX3/FKHR activity by PKC412 also in Rh4 cells.

We found that the inhibitory effect of PKC412 on PAX3/FKHR activity is, at least partially, based on modulation of phosphorylation sites in the PAX3 part of the fusion protein. Nevertheless, it cannot be excluded that also other sites are influenced by PKC412. Whereas phosphorylation of PAX2 (28), PAX6 (29), and PAX8 (30) has been reported, phosphorylation sites in PAX3 have not been identified thus far. However, an influence of PKC on the transcriptional activity of PAX3 in presomitic mesoderm has been suggested in recent work (31). Supporting this observation, we found that PKC412 can inhibit activity of PAX3 in a similar manner to PAX3/FKHR. The region encompassing phosphorylation sites in NterPAX3His described here (peptide 186–216) is located in the linker region between the two DNA-binding domains of PAX3.

Generally, phosphorylation events can regulate the activity of transcription factors via several different mechanisms including changes in subcellular localization, protein stability, DNA-binding activity, and protein-protein interactions. As PKC412 did not influence the nuclear localization of NterPAX3His and even increased the expression level of PAX3/FKHR in 293T cells, we exclude the first two mechanisms as relevant. However, we could show that phosphorylation of the linker region influences PAX3 DNA binding via both the paired domain and the homeodomain. This is in accordance with earlier findings showing an influence of this region on the DNA binding of PAX3 (32).

MALDI-TOF analysis revealed that at least four of six serine residues are phosphorylated in the peptide 186 to 216 of NterPAX3His. Interestingly, only multiple but not single mutations of these sites into aspartate reduced the sensitivity of the protein toward PKC412, suggesting that a combination of several phosphorylated sites is necessary for full transcriptional activity of PAX3/FKHR. Whether all or a combination of some of these sites is involved in PKC412 sensitivity is under current investigation. Furthermore, the fact that exchange of all the six serine residues by aspartate did not completely protect from PKC412-mediated inhibition of PAX3/FKHR suggests that, besides modulation of these phosphorylation sites, other mechanisms regulating PAX3/FKHR activity might be affected by PKC412.

Translocation-positive aRMS cells have been shown to highly depend on the presence of active fusion proteins, as silencing of PAX3/FKHR by oligonucleotides (7) or siRNA (8) very efficiently induces apoptosis in these cells. This suggests that reduction of PAX3/FKHR activity by PKC412 in aRMS cells may be, at least in part, the responsible mechanism for induction of apoptosis. However, taking into account its broad inhibitory spectrum, it cannot be excluded that some of its proapoptotic effects in aRMS cells are based on other mechanisms. As tumors have many, and often overlapping, biological pathways they can use to grow and resist death, inhibition of different signal transduction pathways in parallel may be even more effective when compared with therapies targeting specifically one single pathway (see ref. 33 for review). Hence, inhibition of multiple signaling pathways by PKC412 could be of clinical advantage. Furthermore, such multitargeted therapy is thought to have an increased likelihood of sustained effectiveness due to the reduced probability for appearance of resistant clones.

About one third of the known cellular oncogenes are transcription factors (3, 34); therefore, these factors are highly interesting targets for potential therapeutic interventions. Unfortunately, the absence of a directly targetable enzymatic activity complicates targeting of these factors. Experimental approaches to inhibit transcription factors, such as antisense nucleic acid approaches, are very useful *in vitro*, also in the case of aRMS (7), but the technical complexity of an application *in vivo* prevents routine clinical implementation for the moment. As shown in our study, the use of small-molecule kinase inhibitors influencing transcription factor activity could be an alternative. As most of the ~1,000 human transcription factors are thought to be regulated by phosphorylation (35), the principles shown here may be worthwhile to explore in additional tumors addicted to oncogenic transcription factors (e.g., Ewing's sarcoma).

In summary, our data reveal a novel mechanism regulating PAX3/FKHR activity and at the same time suggest PKC412 as an interesting potential agent for the treatment of aRMS, providing a preclinical rationale for clinical studies with this inhibitor in aRMS patients.

Acknowledgments

Received 6/29/2007; revised 2/20/2008; accepted 3/24/2008.

Grant support: Swiss National Science Foundation grants 3100-067841 and 3100-109837 (B.W. Schäfer). Swiss Research Foundation Child and Cancer.

The costs of publication of this article were defrayed in part by the payment of page charges. This article must therefore be hereby marked *advertisement* in accordance with 18 U.S.C. Section 1734 solely to indicate this fact.

We thank Prof. F.G. Barr for providing constructs with the PAX3/FKHR mutants G48S and N269A, Prof. M. Busslinger for providing 6×CD19 and P3 luciferase constructs, Prof. R.H. Medema for providing the bim-luciferase construct, and Dr. W. Jochum for his help with Ki-67 stainings of tumor sections.

References

1. Sawyers C. Targeted cancer therapy. Nature 2004;432:294–7.
2. Jabbour E, Cortes J, Kantarjian H. Novel tyrosine kinase inhibitors in chronic myelogenous leukemia. Curr Opin Oncol 2006;18:578–83.
3. Futreal PA, Coin L, Marshall M, et al. A census of human cancer genes. Nat Rev Cancer 2004;4:177–83.
4. Merlino G, Helman LJ. Rhabdomyosarcoma—working out the pathways. Oncogene 1999;18:5340–8.
5. Sorensen PH, Lynch JC, Qualman SJ, et al. PAX3-FKHR and PAX7-FKHR gene fusions are prognostic indicators in alveolar rhabdomyosarcoma: a report from the Children's Oncology Group. J Clin Oncol 2002;20:2672–9.
6. Raney RB, Anderson JR, Barr FG, et al. Rhabdomyosarcoma and undifferentiated sarcoma in the first two decades of life: a selective review of Intergroup Rhabdomyosarcoma Study Group experience and rationale for Intergroup Rhabdomyosarcoma Study V. J Pediatr Hematol Oncol 2001;23:215–20.
7. Bernasconi M, Remppis A, Fredericks WJ, Rauscher FJ III, Schafer BW. Induction of apoptosis in rhabdomyosarcoma cells through down-regulation of PAX proteins. Proc Natl Acad Sci U S A 1996;93:13164–9.
8. Ebauer M, Wachtel M, Niggli FK, Schäfer BW. Comparative expression profiling identifies an *in vivo* target gene signature with TFAP2β as a mediator of the survival function of PAX3/FKHR. Oncogene 2007;26:7267–81.
9. Ayyanathan K, Fredericks WJ, Berking C, et al. Hormone-dependent tumor regression *in vivo* by an

inducible transcriptional repressor directed at the PAX3-FKHR oncogene. Cancer Res 2000;60:5803–14.
10. Fabbro D, Ruetz S, Bodis S, et al. PKC412—a protein kinase inhibitor with a broad therapeutic potential. Anticancer Drug Des 2000;15:17–28.
11. Stone RM, DeAngelo DJ, Klimek V, et al. Patients with acute myeloid leukemia and an activating mutation in FLT3 respond to a small-molecule FLT3 tyrosine kinase inhibitor, PKC412. Blood 2005;105:54–60.
12. Scholl FA, Betts DR, Niggli FK, Schafer BW. Molecular features of a human rhabdomyosarcoma cell line with spontaneous metastatic progression. Br J Cancer 2000; 82:1239–45.
13. Wachtel M, Frei K, Ehler E, Fontana A, Winterhalter K, Gloor SM. Occludin proteolysis and increased permeability in endothelial cells through tyrosine phosphatase inhibition. J Cell Sci 1999;112:4347–56.
14. Gorg A, Obermaier C, Boguth G, et al. The current state of two-dimensional electrophoresis with immobilized pH gradients. Electrophoresis 2000;21:1037–53.
15. Czerny T, Schaffner G, Busslinger M. DNA sequence recognition by Pax proteins: bipartite structure of the paired domain and its binding site. Genes Dev 1993;7: 2048–61.
16. Xia SJ, Barr FG. Analysis of the transforming and growth suppressive activities of the PAX3-FKHR oncoprotein. Oncogene 2004;23:6864–71.
17. Motta MC, Divecha N, Lemieux M, et al. Mammalian SIRT1 represses forkhead transcription factors. Cell 2004;116:551–63.
18. Wachtel M, Dettling M, Koscielniak E, et al. Gene expression signatures identify rhabdomyosarcoma subtypes and detect a novel t(2;2)(q35;p23) translocation fusing PAX3 to NCOA1. Cancer Res 2004;64: 5539–45.
19. Hosoi H, Dilling MB, Shikata T, et al. Rapamycin causes poorly reversible inhibition of mTOR and induces p53-independent apoptosis in human rhabdomyosarcoma cells. Cancer Res 1999;59:886–94.
20. Begum S, Emani N, Cheung A, Wilkins O, Der S, Hamel PA. Cell-type-specific regulation of distinct sets of gene targets by Pax3 and Pax3/FKHR. Oncogene 2005; 24:1860–72.
21. Propper DJ, McDonald AC, Man A, et al. Phase I and pharmacokinetic study of PKC412, an inhibitor of protein kinase C. J Clin Oncol 2001;19:1485–92.
22. Fabian MA, Biggs WH III, Treiber DK, et al. A small molecule-kinase interaction map for clinical kinase inhibitors. Nat Biotechnol 2005;23:329–36.
23. Fabbro D, Buchdunger E, Wood J, et al. Inhibitors of protein kinases: CGP 41251, a protein kinase inhibitor with potential as an anticancer agent. Pharmacol Ther 1999;82:293–301.
24. Chen J, Deangelo DJ, Kutok JL, et al. PKC412 inhibits the zinc finger 198-fibroblast growth factor receptor 1 fusion tyrosine kinase and is active in treatment of stem cell myeloproliferative disorder. Proc Natl Acad Sci U S A 2004;101:14479–84.
25. Chen J, Lee BH, Williams IR, et al. FGFR3 as a therapeutic target of the small molecule inhibitor PKC412 in hematopoietic malignancies. Oncogene 2005;24:8259–67.
26. Gleixner KV, Mayerhofer M, Aichberger KJ, et al. PKC412 inhibits *in vitro* growth of neoplastic human mast cells expressing the D816V-mutated variant of KIT: comparison with AMN107, imatinib, and cladribine (2CdA) and evaluation of cooperative drug effects. Blood 2006;107:752–9.
27. Bahlis NJ, Miao Y, Koc ON, Lee K, Boise LH, Gerson SL. N-benzoylstaurosporine (PKC412) inhibits Akt kinase inducing apoptosis in multiple myeloma cells. Leuk Lymphoma 2005;46:899–908.
28. Cai Y, Lechner MS, Nihalani D, Prindle MJ, Holzman LB, Dressler GR. Phosphorylation of Pax2 by the c-Jun N-terminal kinase and enhanced Pax2-dependent transcription activation. J Biol Chem 2002; 277:1217–22.
29. Mikkola I, Bruun JA, Bjorkoy G, Holm T, Johansen T. Phosphorylation of the transactivation domain of Pax6 by extracellular signal-regulated kinase and p38 mitogen-activated protein kinase. J Biol Chem 1999;274: 15115–26.
30. Van Renterghem P, Vassart G, Christophe D. Pax 8 expression in primary cultured dog thyrocyte is increased by cyclic AMP. Biochim Biophys Acta 1996; 1307:97–103.
31. Brunelli S, Relaix F, Baesso S, Buckingham M, Cossu G. β Catenin-independent activation of MyoD in presomitic mesoderm requires PKC and depends on Pax3 transcriptional activity. Dev Biol 2007;304: 604–14.
32. Fortin AS, Underhill DA, Gros P. Helix 2 of the paired domain plays a key role in the regulation of DNA-binding by the Pax-3 homeodomain. Nucleic Acids Res 1998;26:4574–81.
33. Faivre S, Djelloul S, Raymond E. New paradigms in anticancer therapy: targeting multiple signaling pathways with kinase inhibitors. Semin Oncol 2006;33: 407–20.
34. Karamouzis MV, Gorgoulis VG, Papavassiliou AG. Transcription factors and neoplasia: vistas in novel drug design. Clin Cancer Res 2002;8:949–61.
35. Gardner KH, Montminy M. Can you hear me now? Regulating transcriptional activators by phosphorylation. Sci STKE 2005;2005:pe44.

Phosphorylation Regulates Transcriptional Activity of PAX3/FKHR and Reveals Novel Therapeutic Possibilities

Ralf Amstutz, Marco Wachtel, Heinz Troxler, et al.

Cancer Res 2008;68:3767-3776.